

Evidence Suggesting That Discontinuous Dosing of ALK Kinase Inhibitors May Prolong Control of ALK⁺ Tumors

Amit Dipak Amin¹, Soumya S. Rajan², Winnie S. Liang^{3,4}, Praechompoo Pongtornpipat¹, Matthew J. Groysman⁵, Edgar O. Tapia², Tara L. Peters², Lori Cuyugan^{3,4}, Jonathan Adkins^{3,4}, Lisa M. Rimsza⁶, Yves A. Lussier^{1,7,8}, Soham D. Puvvada⁷, and Jonathan H. Schatz^{1,7,9}

Abstract

The anaplastic lymphoma kinase (ALK) is chromosomally rearranged in a subset of certain cancers, including 2% to 7% of non-small cell lung cancers (NSCLC) and ~70% of anaplastic large cell lymphomas (ALCL). The ALK kinase inhibitors crizotinib and ceritinib are approved for relapsed ALK⁺ NSCLC, but acquired resistance to these drugs limits median progression-free survival on average to ~10 months. Kinase domain mutations are detectable in 25% to 37% of resistant NSCLC samples, with activation of bypass signaling pathways detected frequently with or without concurrent ALK mutations. Here we report that, in contrast to NSCLC cells, drug-resistant ALCL cells show no evidence of bypassing ALK by activating alternate signaling pathways. Instead, drug resistance selected in this setting reflects

upregulation of ALK itself. Notably, in the absence of crizotinib or ceritinib, we found that increased ALK signaling rapidly arrested or killed cells, allowing a prolonged control of drug-resistant tumors *in vivo* with the administration of discontinuous rather than continuous regimens of drug dosing. Furthermore, even when drug resistance mutations were detected in the kinase domain, overexpression of the mutant ALK was toxic to tumor cells. We confirmed these findings derived from human ALCL cells in murine pro-B cells that were transformed to cytokine independence by ectopic expression of an activated NPM-ALK fusion oncoprotein. In summary, our results show how ALK activation functions as a double-edged sword for tumor cell viability, with potential therapeutic implications. *Cancer Res*; 75(14); 2916–27. ©2015 AACR.

Introduction

ALK is a receptor tyrosine kinase expressed in the developing nervous system (1, 2). Chromosomal rearrangements in subsets of several cancers result in constitutive expression and activation of its C-terminal kinase domain, which prolifically turns on oncogenic signaling pathways, including JAK3/STAT3, MEK/ERK, and PI3K/AKT (3–6). Addition of tumor cells to ALK activity in laboratory models and promising activity of ALK inhibition in early-phase clinical trials have made it an intensive target for TKI development in recent years. ALK originally was cloned from the

recurrent t(2;5)(p23;q35) chromosomal rearrangement found in anaplastic large-cell lymphoma (ALCL), an uncommon tumor derived from mature T cells (7). The resulting NPM-ALK fusion kinase and other less common ALK fusions drive malignant growth in ~70% of ALCL cases. Though identified in ALCL 20 years ago, ALK has only become a target for intensive drug development since 2007, when its presence was discovered in a subset of non-small cell lung cancer (NSCLC). Here, activation is again through chromosomal rearrangement creating an expressed and activated fusion kinase, most commonly EML4-ALK (8, 9).

Such rearrangements are present in 2% to 7% of NSCLC cases and led to a 57% response in phase 1 evaluation of the first-in-class ALK TKI crizotinib in relapsed ALK⁺ NSCLC patients (10). The drug won accelerated limited FDA approval in 2011 and subsequently promoted longer progression-free survival than chemotherapy as first or second-line treatment for metastatic ALK⁺ NSCLC (11, 12). The second-generation inhibitor ceritinib (LDK378) was approved recently for crizotinib-resistant ALK⁺ NSCLC patients based on a 58% response rate in phase 1, including 56% response in patients with prior crizotinib exposure (13), and several other ALK TKIs are under development (14). ALCL, meanwhile, which makes up 2% to 5% of non-Hodgkin lymphoma (NHL), is the most common T-cell NHL in children and the third most common in adults. Although ALK⁺ ALCL has better response to chemotherapy than other peripheral T-cell lymphomas (15), poor prognosis of relapsed or refractory patients and its predilection for younger populations have prompted clinical investigation of ALK tyrosine kinase inhibition in both adults and children with the disease (16, 17).

¹BIO5 Institute, University of Arizona, Tucson, Arizona. ²Cancer Biology Graduate Interdisciplinary Program, University of Arizona, Tucson, Arizona. ³Integrated Cancer Genomics Division, Translational Genomics Research Institute, Phoenix, Arizona. ⁴Neurogenomics Division, Translational Genomics Research Institute, Phoenix, Arizona. ⁵Undergraduate Biology Research Program, University of Arizona, Tucson, Arizona. ⁶Department of Pathology, University of Arizona, Tucson, Arizona. ⁷Department of Medicine, University of Arizona, Tucson, Arizona. ⁸Statistics Graduate Interdisciplinary Program, University of Arizona, Tucson, Arizona. ⁹Department of Pharmacology and Toxicology, University of Arizona, Tucson, Arizona.

Note: Supplementary data for this article are available at Cancer Research Online (<http://cancerres.aacrjournals.org/>).

Corresponding Author: Jonathan H. Schatz, University of Arizona Cancer Center, 1515 N. Campbell Avenue, Tucson, AZ 85724. Phone: 520-626-0191; Fax: 520-626-2225; E-mail: schatzj@email.arizona.edu

doi: 10.1158/0008-5472.CAN-14-3437

©2015 American Association for Cancer Research.

Studies of resistance to crizotinib in NSCLC identify target-dependent mechanisms such as kinase-domain mutations and fusion-ALK copy-number gains in 34% to 46%; resistant cases also show frequent activation of known alternate NSCLC drivers such as c-KIT, EGFR, or KRAS, both with and without concurrent ALK mutations, whereas many cases are resistant for unclear reasons (14, 18, 19). Here, we studied resistance to ALK-kinase inhibition in ALK⁺ ALCL using both crizotinib and ceritinib. In contrast to findings in lung cancer, our study identified no ability of ALCL cells to bypass the driver kinase by activation of alternate pathways. Instead, cells upregulated NPM-ALK expression through genomic amplification and other mechanisms, suggesting a nearly absolute addiction to ALK-kinase activity. Strikingly, however, withdrawal of ALK inhibitor from resistant cells causes rapid growth arrest followed by entry into apoptosis, which promoted regression of tumors *in vivo*.

Materials and Methods

Cell lines and reagents

All lines except FL5.12 were purchased from DSMZ, authenticated by STR-fingerprinting (last tested 11/2013) and mycoplasma tested by Plasmotest kit (Invivogen; REP-PT1). Culture media for Karpas-299, SU-DHL-1, MAC-2A: RPMI 1640, 10% fetal bovine serum (FBS), penicillin/streptomycin (P/S); SUP-M2: same but 20% FBS; Phoenix: DMEM, 10% FBS, P/S. FL5.12 cells (gift of Hans-Guido Wendel, Memorial Sloan Kettering Cancer Center, New York, NY): RPMI 1640, 10% FBS, P/S, \pm 10% WeHi-3B supernatant and murine IL3 (400 pmol/L; eBioscience).

Antibodies

Cell Signaling Technology: ALK (#3333S), pALK-Y1604 (3341S), AKT (#4685S), pAKT-S473 (#4060S), ERK1/2 (#4695S), pERK1/2-T202/Y204 (#4370S), STAT3 (#4904S) and pSTAT-Y705 (#9145S). Sigma: horseradish peroxidase-conjugated anti-rabbit secondary (#A0545), horseradish peroxidase-conjugated anti-mouse secondary (#A9917), α -tubulin (#T9026).

Inhibitors

Crizotinib (PF-02341066; #S1068) was purchased from Selleck Chemicals. Ceritinib (LDK378) kindly provided by Novartis.

Long insert whole genome sequencing

Long insert whole genome sequencing was carried out as described (20), utilizing genomic DNA extracted using the AllPrep DNA/RNA Mini Kit (QIAGEN #80204).

Apoptosis assays

Nexin reagent (Millipore #4500-0455) by the manufacturer's instructions using the Guava EasyCyte flow cytometer.

Cell viability assays

Cells were seeded at 3,000 per well with serial dilutions of indicated inhibitors. Viability was assessed at 72 hours unless otherwise indicated with Cell Titer Glo reagent (Promega #G7573) by the manufacturer's protocol. Luminescence measured by BioTek Synergy HT plate reader. IC₅₀s were calculated with nonlinear curve-fit regression in GraphPad Prism version 6.

Proliferation assays and imaging

Cells were plated at 100,000/mL on day 0 and counted using Trypan-blue exclusion. Cells were stained with Hoechst (1:5,000; Invitrogen #33342) and imaged using the DeltaVision Core system (Applied Precision) equipped with an Olympus IX71 microscope, a 40 \times objective (NA 1.35) and a 20 \times objective (NA 0.70), and a cooled charge-coupled device camera (CoolSNAP HQ2; Photometrics). Images were acquired with softWoRx v1.2 software (Applied Science).

Protein extraction, quantification, and immunoblotting

Cells were seeded at 500,000/mL and incubated as indicated. Proteins were extracted using RIPA (50 mmol/L Tris-HCL pH 8.0, 150 mmol/L NaCl, 1% NP40, 0.5% sodium deoxycholate, and 0.1% SDS), 7 \times phosphatase inhibitor (Roche #04693159001), Phosphatase Halt (Thermo #78428), and Triton X-100. Proteins were quantified using the BCA Assay (Thermo #23225) with 30 μ g loaded per lane for Western blotting. All blots were developed using autoradiography film (GeneMate #F-9023-8 \times 10) after incubation with antibodies indicated above.

Copy-number assays

Genomic DNA was extracted by AllPrep DNA/RNA Mini Kit (QIAGEN #80204). Copy-number probes for NPM1 exon 1 (#Hs01219772_cn), NPM intron 11 (#Hs06724352_cn), ALK intron 1 (#Hs05853206_cn), ALK intron 23 (#Hs04555433_cn), and TERT (#4401633) were purchased from Life Technologies, and assays were conducted per the manufacturer's instructions. Copy-number analysis was by Applied Biosystems Prism 7000 Sequence Detection System. Data were normalized to the house-keeping gene (TERT) and analyzed using the 2^{- $\Delta\Delta$ Ct} method.

qRT-PCR

RNA isolation by RNeasy Mini Kit (QIAGEN #74106); cDNA generated by Taqman Reverse Transcriptase Kit (Roche; #N808-0234) on a Bio-Rad T100 Thermal Cycler. qRT-PCR employed an Applied Biosystems Prism 7000 Sequence Detection System with Taqman probes (Life Technologies): NPM-ALK (#Hs03024829_ft), CDKN2A (#Hs00923894_m1), and GAPDH as endogenous control (#Hs02758991_g1). Data were analyzed using the 2^{- $\Delta\Delta$ Ct} method.

Targeted selection and sequencing of the expressed NPM1-ALK translocation locus

cDNA was synthesized from 100 ng total RNA using the Nugen Ovation RNA-Seq System v2. Presence of NPM-ALK confirmed by PCR giving a 429bp product (Kapa Biosystem's HiFi Ready-mix; #KK1006) using previously published primers flanking the breakpoint (21). NPM1-ALK fusion cDNA was then amplified using the QIAGEN Long Range PCR Kit (#206401) and custom primers (F1: GTCCGCCTTCTCTCTACCT, R1: TTGGCA-CAAAACAAAACGGT) flanking the breakpoint, encompassing 391bp of NPM1 and 1804bp of ALK cDNA. Size selection and purification of the PCR product using Bio-Rad's Freeze 'N' Squeeze DNA gel extraction spin columns (#4106139) followed by Beckman Coulter Agencourt AMPure XP Bead purification (#A63880). A total of 50 ng of each PCR product was fragmented to 300bp using the Covaris E210 sonicator, and libraries were constructed using Kapa Biosystems' Hyper Kit (#KK8504) following the manufacturer's protocol. Libraries

Amin et al.

were equimolarly pooled and sequenced on the Illumina MiSeq for paired 84bp reads using Illumina's MiSeq Reagent Kit v3 (#MS-102-3001). FASTQ files generated from the Illumina MiSeq were aligned against build 37 of the human reference genome using the Burrows-Wheeler Alignment (BWA) tool (22). Following alignment, .sai files were used to create .sam (sequence alignment map) files, which were used to create binary sequence (.bam) files using SAMtools (23). PCR duplicates were flagged for removal using Picard (<http://picard.sourceforge.net>), and base quality scores were recalibrated using Genome Analysis Toolkit (GATK; ref. 24). Comparisons within each cell line family were performed to identify point mutations and small indels using three somatic callers, including Seurat (25), MuTect (26), and Strelka (27) as well as Sanger sequencing.

Transfections, infections, and selection

Phoenix packaging cells were seeded at 700,000 cells/mL for 16 hours, to which, a cocktail of DMEM, X-treme GENE 9 DNA transfection reagent (Roche #06365787001) and 1 μ g MIG-NPM-ALK was added drop-wise. This mixture was incubated for 48 hours to allow production of viral supernatant. A total of 100,000 murine pro-B 5-12 cells were then resuspended in 600 μ L of syringe-filtered viral supernatant mixed with 150 μ L of a 5 \times infection solution (WeHi-3B, Polybreen, and interleukin-3). This was repeated a further three times with at least 6 hours between each repeat to allow viral supernatant to reach maximum titer. Cells were then plated in RPMI 1640 media supplemented with 10% FBS, P/S, 10% WeHi-3B supernatant, and interleukin-3 for 24 hours and assessed by FACS (using the Guava EasyCyte flow cytometer) for GFP levels as a mark of initial infection. Cytokine withdrawal was carried out by washing cells in RPMI 1640 media supplemented with 10% FBS and P/S four times and subsequently plating them in this cytokine-free media with 1:1,000 DMSO or the indicated ceritinib concentrations. FACS plots were analyzed using FlowJo version 10.

Xenograft experiments

All mouse experiments were approved by the University of Arizona Animal Care and Use Committee (protocol no. 12-377). Mice were maintained under specific pathogen-free conditions, and food and water were provided *ad libitum*.

In vivo dependence

Severe combined immunodeficiency (SCID) mice were injected with 2×10^6 K299-CR1000 cells in 1:1 Matrigel and sterile saline in a total volume of 100 μ L subcutaneously into the lower flank. These mice were divided immediately to two groups for treatment with ceritinib or vehicle by oral gavage. Ceritinib was formulated freshly before each dosing as a solution in 0.5% MC (methylcellulose)/0.5% Tween 80 as described (28). Because of the requirement for ALK inhibition for K299-CR1000 cells *in vitro*, dosing began on the day of flank injections 2 hours before hand and continued daily.

Up-front intermittent versus continuous dosing

SCID mice were injected with 2×10^6 Karpas-299 parental cells as above. After tumors reached ~ 500 mm³, the mice were split into seven cohorts ($n = 3$) and were treated continuously with vehicle, continuously with ceritinib (at either 33.33 or 50 mg/kg) or intermittently with the same concentrations of ceritinib using a '4 weeks on, 2 weeks off' schedule.

Statistical analysis

Two-tailed Student *t* test was carried out for all expression data using the GraphPad *t* test calculator and verified using the SPSS Statistics software from IBM, with $P < 0.05$ considered statistically significant with a 95% confidence interval. Apoptosis data were calculated using the Mann-Whitney test in GraphPad where $P = 0.05$ was considered statistically significant with a 95% confidence interval.

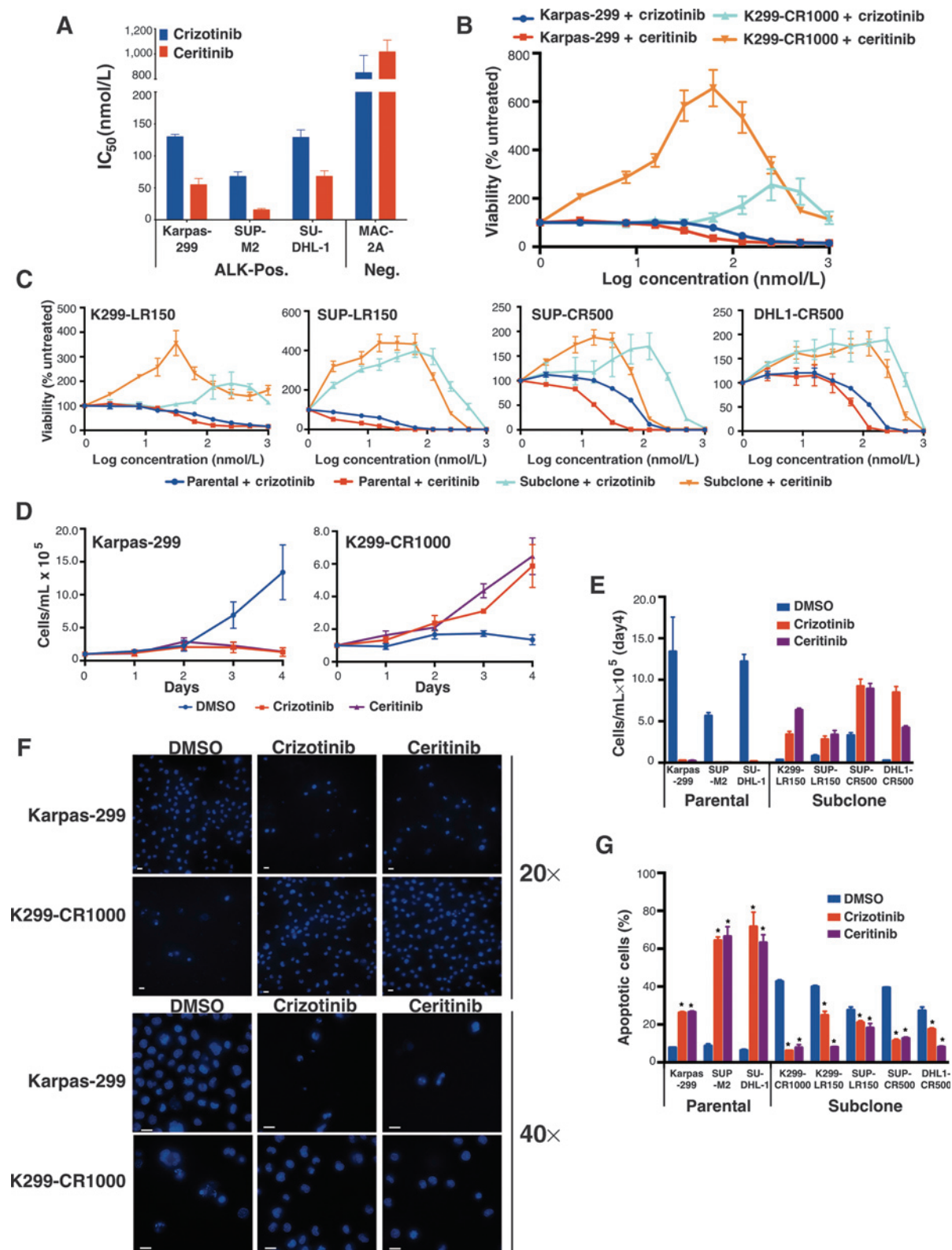
Results

TKI resistance and dependence are invariably coselected in ALK⁺ ALCL

NPM-ALK-driven ALCL cell lines Karpas-299, SU-DHL-1, and SUP-M2 were highly sensitive to crizotinib and ceritinib, with the latter drug having 3 to 5 \times greater potency (Fig. 1A; Supplementary Table S1). We selected for resistance to both inhibitors independently through serial plating in increasing drug concentrations (Supplementary Fig. S1A). Cells derived from Karpas-299 able to grow in 1,000 nmol/L crizotinib (hereafter K299-CR1000) strikingly when washed out of ALK inhibitor and reassessed for drug sensitivity showed viability stimulation by both inhibitors (Fig. 1B). Stimulation was an on-target effect, indicated by the stimulation at lower concentration by the more potent inhibitor. All resistant clones emerging from selections demonstrated similar findings [Fig. 1C, lines named for parent, drug used in selection (L for ceritinib/LDK378), and top nanomolar concentration]. When washed out of inhibitor and plated in drug-free media, resistant cells halted growth, suggesting ALK inhibition had become a requirement for viability (Fig. 1D-E). Plated without ALK inhibitor, resistant lines appeared shrunken and involuted, consistent with onset of apoptosis, while those in either ALK inhibitor appeared viable similar to parent cells growing without drug (Fig. 1F; Supplementary Fig. S1B). Flow cytometry confirmed entry into apoptosis by resistant cells plated in drug-free media, in contrast to those maintained in either ALK inhibitor (Fig. 1G). ALK⁺ ALCL cells therefore reliably develop ALK-inhibitor dependence at the same time they develop resistance, suggesting selection for a process with paradoxical effects on viability.

NPM-ALK upregulation drives both resistance and dependence

To investigate the resistant-dependent phenotype, we performed long-insert whole-genome sequencing (LI-WGS; ref. 20) of the Karpas-299 parent line and the K299-CR1000 subclone. Mapping of reads against the reference genome (hg19) showed amplification in the subclone of the portions of the *NPM* and *ALK* loci that are translocated to form *NPM-ALK* (Fig. 2A). Copy-number assays demonstrated gain consistent with genomic amplification specifically of the fusion locus but not the uninvolved portions of either gene (Fig. 2B). This generated more than 50-fold increased expression of *NPM-ALK* mRNA (Fig. 2C). The additional resistant-dependent subclones also had increased expression relative to their corresponding parent lines (Fig. 2D), ranging from 1.5 \times for SUP-LR150 to 12.0 \times for K299-LR150. Of these, only K299-LR150 had clear evidence of *NPM-ALK* copy-number gain (Supplementary Fig. S2), demonstrating increased expression results also from other mechanisms. *NPM-ALK* protein levels also were elevated in subclones (Fig. 2E). This is seen at *NPM-*

**Figure 1.**

TKI resistance dependence in ALK⁺ ALCL. A, initial sensitivities to ALK inhibition (see also Supplementary Figure S1 for timelines acquired resistance). B and C, stimulation of viability by both ALK inhibitors in cells with acquired resistance. D and E, proliferation of parent and subclonal cells seeded at 10⁵/mL in media with DMSO, crizotinib, or ceritinib. F, Hoechst-stained cells from D on Day 4 (scale bars, 15 μm). G, combined early/late apoptotic cells from D to E at day 4 by flow cytometry. Means of technical quadruplicates (A–C) or independent triplicates (D, E, G) ±SEM. **P* = 0.05 (Mann-Whitney).

Amin et al.

ALK's full-length position (80 kDa) and at a prominent high molecular weight aggregate band known to result from elevated NPM-ALK protein levels (29). Activating ALK auto-phosphorylation, highly drug sensitive in parent lines, was drug resistant in subclones during TKI exposure. STAT3 activation previously was shown to be required for ALK-mediated lymphomagenesis (30). In addition, the gene-expression signature of clinical cases is most similar to that of a STAT3 survival signature (31). We found all resistant subclones preserved STAT3 phosphorylation during ALK inhibitor exposure in marked contrast to the drug-sensitive parent lines (Fig. 2E). Subclones withdrawn from drug showed increase in ALK and STAT3 phosphorylation but, interestingly, slight but noticeable decline in total STAT3, suggesting feedback repression of

STAT3 expression. In sum, increased ALK expression drives resistance associated with preserved STAT3 activation but leads to increased ALK signaling when drug is withdrawn. This combined with the rescue of cell viability by ALK inhibition (Fig. 1) supports a conclusion that ALK overdose is the reason for growth arrest and apoptosis upon inhibitor withdrawal.

We also performed both Sanger and targeted deep sequencing of the *NPM-ALK* fusion locus (Supplementary Table S2). Neither K299-CR1000 nor K299-LR150 cells developed any second-site kinase-domain mutations. Resistance in these lines therefore was driven purely by increased NPM-ALK levels. The same may be true of DHL1-CR500, which acquired only R1192P, a germline predisposition allele for neuroblastoma with no known role in TKI resistance (32). Intriguingly, both SUP-CR500 and SUP-LR150

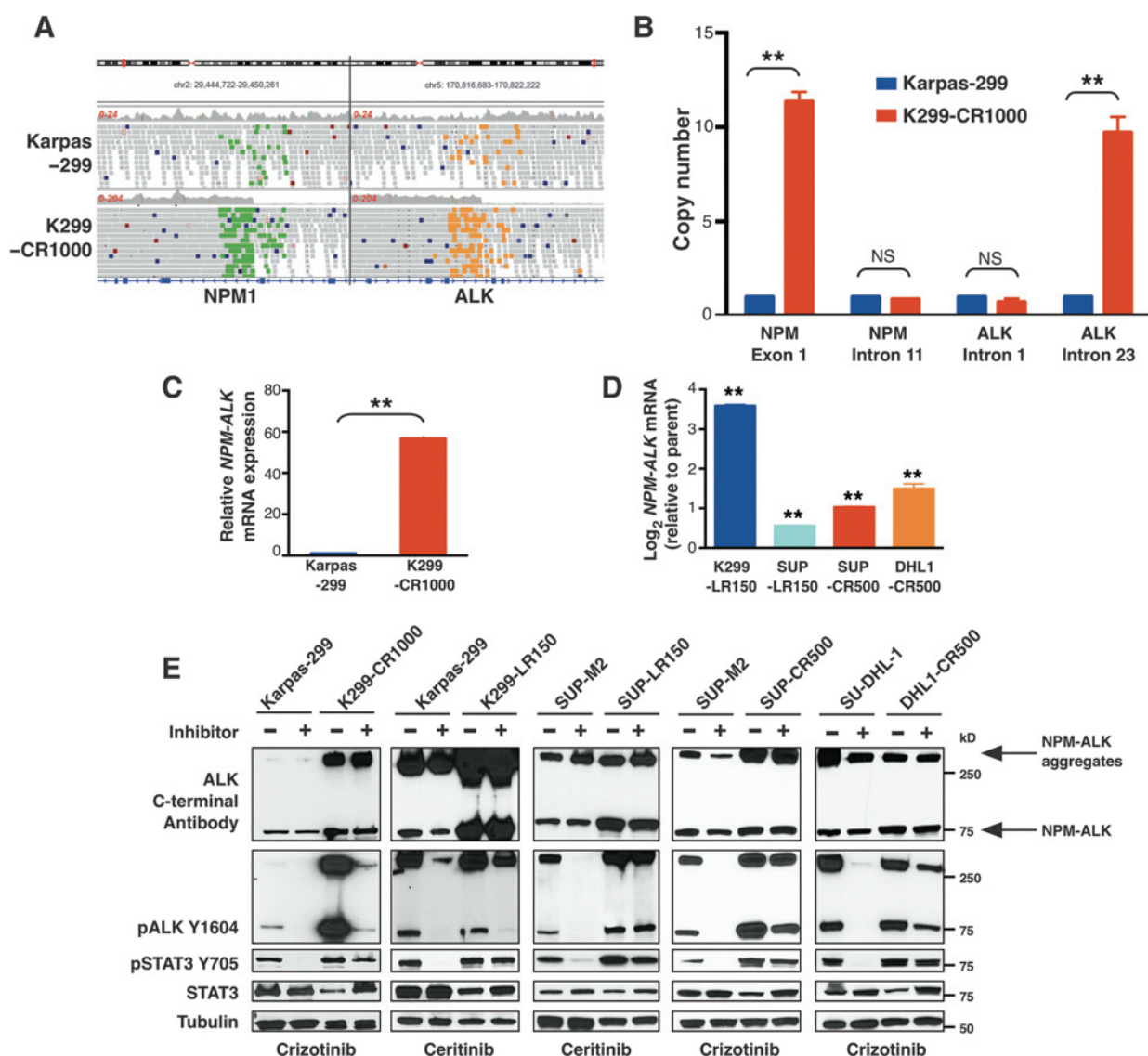


Figure 2.

NPM-ALK upregulation drives resistance dependence. A, LI-WGS reads indicate *NPM-ALK* amplification in resistant-dependent subclone. B, copy-number assay confirms gain specifically of the fusion kinase-encoding regions of *NPM* and *ALK* (see also Supplementary Fig. S2 for additional resistant cells). C and D, increased *NPM-ALK* mRNA expression in subclones. E, immunoblotting with and without crizotinib in parent and subclones. Means of technical triplicates (B-D) \pm SEM. ** $P < 0.01$; * $P < 0.05$; NS, nonsignificant, $P \geq 0.05$ (t test).

developed mutations with known roles in TKI resistance (respectively I1171S, seen only by Sanger sequencing, and F1174L, seen by both targeted and Sanger sequencing; Supplementary Table S2; refs. 33–36). The fact that these lines also developed ALK upregulation leading to TKI dependence to avoid signaling overdose further illustrates the intense pressure for these systems to acquire target-dependent resistance. Moreover, a treatment strategy designed to exploit ALK overdose such as discontinuous dosing may be at least temporarily successful even when drug-specific kinase-domain mutations also have begun to arise.

ALK overdose also impairs the fitness of cytokine-dependent pro-B cells

To replicate resistance-dependence in an independent system, we employed the FL5.12 line, murine pro-B cells that rapidly cease proliferating and undergo apoptosis without IL3 (37). We created NPM-ALK-dependent FL5.12 lines through retroviral introduc-

tion of NPM-ALK with GFP coexpression followed by IL3 withdrawal. We hypothesized simultaneous IL3 withdrawal and ALK-inhibitor exposure would require progressively higher NPM-ALK levels to permit survival in the presence of drug. Figure 3A shows representative percentage GFP enrichment in one of three replicate experiments 4 days after IL3 withdrawal and incubation in 0, 10, 20, 50, 150, or 500 nmol/L ceritinib. Confirming NPM-ALK dependence, cells withdrawn in the two highest concentrations always died, whereas the others proliferated only as 100% GFP⁺ lines. In addition, cells infected with empty vector invariably perished after IL3 withdrawal (not shown). Flow-cytometry analysis showed progressively brighter GFP coexpression in the transformed cells selected and maintained in higher ceritinib concentrations (Fig. 3B), and qPCR confirmed increased NPM-ALK mRNA (Fig. 3C). By immunoblot, we observed progressively higher NPM-ALK total protein and phosphorylation, showing again selection for increased ALK expression and activity to permit survival of NPM-ALK-dependent cells during TKI exposure (Fig.

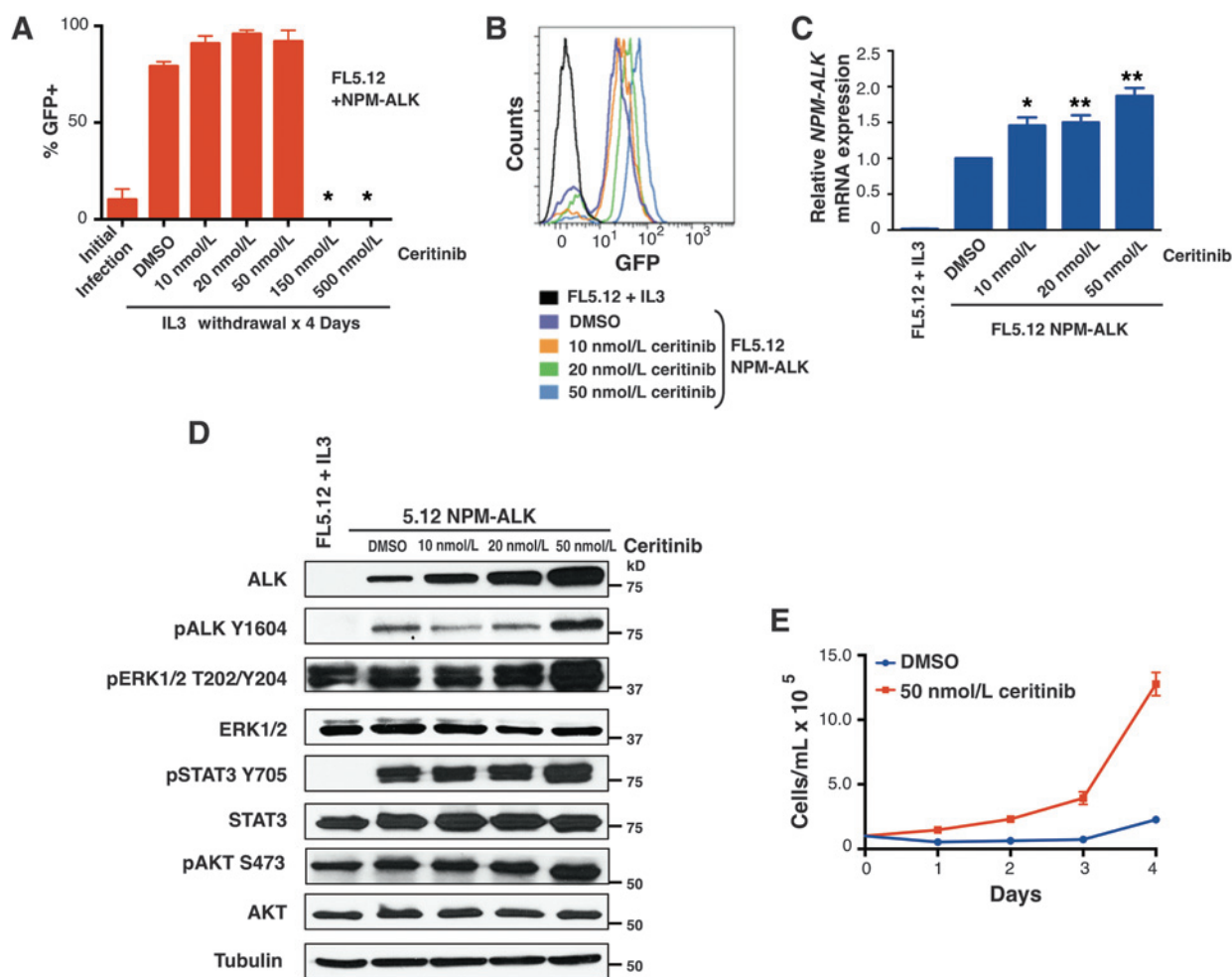


Figure 3.

ALK upregulation drives resistance dependence in transformed pro-B cells. A, retroviral introduction of NPM-ALK in a GFP coexpressing vector-transformed FL5.12 cells to cytokine independence with simultaneous ceritinib incubation. *, cells did not survive. B, GFP intensity by ceritinib concentration. C and D, NPM-ALK mRNA and protein expression with increasing ceritinib concentration. E, proliferation in cytokine-free media of FL5.12/NPM-ALK cells transformed with 50 nmol/L ceritinib co-incubation, with and without drug. Means of technical quadruplicates (C) and independent triplicates (A, D, E, and F) \pm SEM. ** $P < 0.01$; * $P < 0.05$; NS, nonsignificant, $P \geq 0.05$ (t test).

Amin et al.

3D). We then washed cells selected and maintained in 50 nmol/L crizotinib out of drug, plated them in drug-free media, and compared their proliferation with the same cells maintained in drug. The cells deprived of drug had significantly reduced proliferation (Fig. 3E). Therefore, an independent system confirmed both selection for increased NPM-ALK expression to mediate TKI resistance and the negative impact on cell fitness of this increased expression in TKI absence.

Cells return NPM-ALK to basal levels to permit growth without ALK inhibition

To identify factors permitting resistant-dependent cells to resume growth without ALK inhibition, we attempted to derive lines with this phenotype *in vitro*. Invariably, plating resistant cells at $<10^6$ /mL without ALK inhibitor resulted in complete death of the culture plate (data not shown). At concentrations $\geq 10^6$ /mL, however, we eventually isolated clones from resistant-dependent

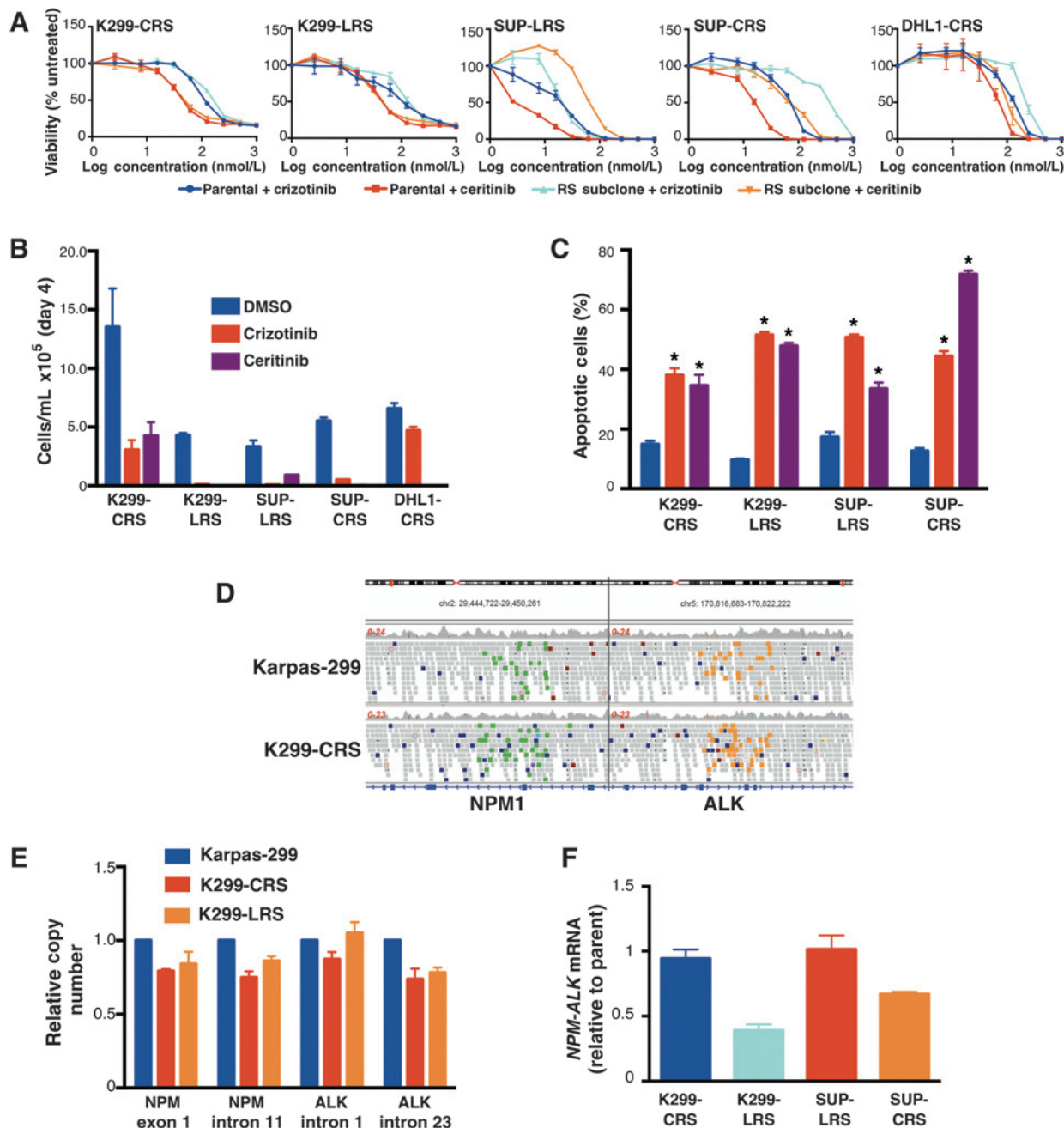


Figure 4.

Proliferation with TKIs requires return of ALK to baseline. A, resensitized (RS) cell viability in response to ALK inhibition, with original parent lines for comparison. B and C, RS proliferation (B) and apoptosis (C) on day 4 after seeding at 10^5 /mL in media containing DMSO, crizotinib, or ceritinib. D and E, LI-WGS (D) and qPCR copy-number assays (E) show no amplification of *NPM-ALK* in K299 RS subclones. F, mRNA expression relative to original parent. See also Supplementary Fig. S3 (for protein analysis). Means of technical quadruplicates (A) or technical triplicates (B, C, E, and F) \pm SEM.

lines able to again grow in drug-free media (Supplementary Fig. S1, range 4–56 days). Designated RS for resensitized (K299-CRS, K299-LRS, SUP-CRS, and SUP-LRS), these lines lacked viability stimulation by either ALK inhibitor (Fig. 4A). Proliferation assays showed ability to grow again without drug but resensitization to both ALK inhibitors in all RS lines (Fig. 4B). The RS lines, like parent cells, were less apoptotic in drug-free media than in either ALK inhibitor (Fig. 4C). These clones therefore lost ability to proliferate in ALK TKIs as they regained ability to grow without drug. [Note: ALK TKI resistance mutations detected in SUP-CRS and SUP-LRS (Supplementary Table S2), which likely shifted their viability curves compared with parent cells in Fig. 4A, were not sufficient to restore proliferation or avoid apoptosis during drug exposure.] LI-WGS of K299-CRS showed no genomic amplification of *NPM-ALK* (Fig. 4D), and copy-number assays showed K299-CRS and K299-LRS have the *NPM-ALK* translocation at the same copy-number as the original parent (Fig. 4E). The RS subclones all returned *NPM-ALK* mRNA (Fig. 4G) and protein (Supplementary Fig. S3) to approximately the same levels as those in the corresponding original parent cells. Return of ALK activity to baseline therefore appears necessary for resistant subclones to resume proliferation in an absence of an ALK inhibitor. Simultaneous resensitization to drug that results from this return to baseline strongly validates the conclusion that ALK overdose drives both resistance to and dependence on TKIs.

We also re-selected K299-CRS cells for crizotinib resistance and obtained a secondary resistant clone able to grow at 1,000 nmol/L (K299-CR1000-2). Strikingly, the resistance selection took just as long as the original selection of Karpas-299 cells and again resulted in *NPM-ALK* copy-number gain, increased mRNA expression, and the resistant-dependent phenotype (Supplementary Fig. S4). Again no mutations were acquired within the ALK kinase domain (Supplementary Table S2). This further demonstrates the great difficulty ALK⁺ ALCL cells have in gaining an ALK-independent means of survival.

ALK overdose prevents tumor engraftment without TKI treatment *in vivo* and permits prolonged tumor control through discontinuous dosing

Our data suggest withdrawal of drug from ALK⁺ ALCL patients with TKI resistance due to target upregulation may promote tumor regression due to ALK overdose. We therefore xenografted K299-CR1000 cells to SCID mice, immediately began treatment with vehicle or ceritinib (50 mg/kg, *n* = 5 per group), and followed tumor volume (Fig. 5A). No vehicle-treated animals experienced tumor engraftment, whereas three of five ceritinib animals did. On day 62, we discontinued ceritinib treatment, resulting in tumor regression in all engrafted mice (Fig. 5B). Tumors began growing again, however, after about 25 days. We followed them until the tumor burden of one mouse approached 2,000 mm³, at which point we took tumor samples for *in vitro* culture and then resumed ceritinib therapy. We successfully cultured the cells from two of the three mice. Strikingly, cells from both animals had all the characteristics of the *in vitro* RS subclones (Fig. 4), including no viability stimulation by either ALK TKI (Fig. 5C), ability to proliferate in vehicle but not either ALK inhibitor (Fig. 5D), loss of the *NPM-ALK* copy-number gain (Fig. 5E), and return of *NPM-ALK* mRNA expression to the baseline of the original

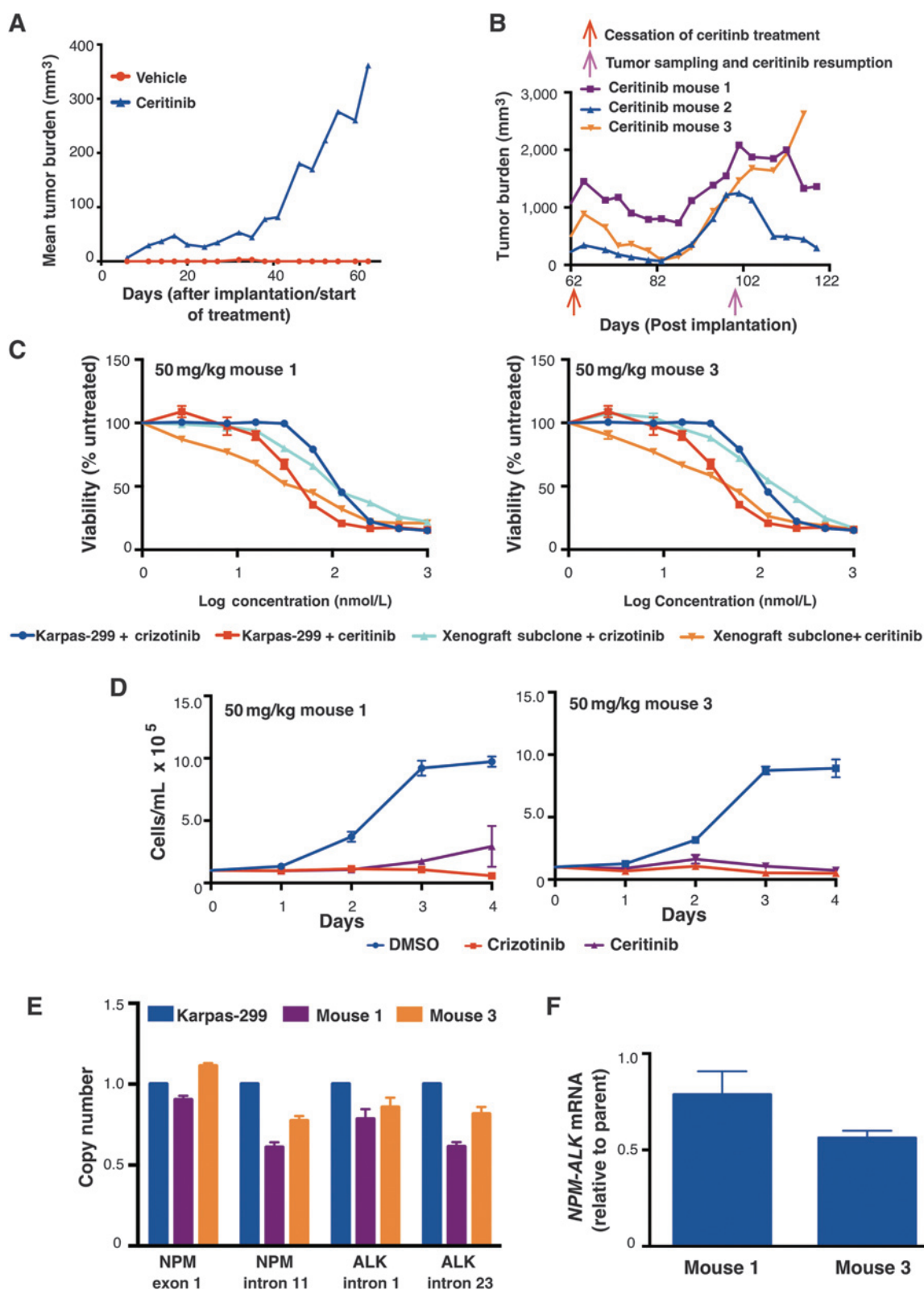
Karpas-299 parent line (Fig. 5F). Consistent with resensitization, ceritinib resumption halted the growth of tumors in all three mice, with two experiencing tumor reduction over the next 22 days when the experiment ended (Fig. 5B). The third tumor began growing again after 12 days despite the ongoing ceritinib therapy. These results show proof of principle that discontinuous dosing *in vivo* can take cells through full cycles of ALK TKI dependence and sensitivity and can prolong tumor control in host animals bearing tumors with resistance driven by ALK overexpression. Up-front comparison of intermittent versus continuous in SCID mice engrafted with parental Karpas-299 xenografts did not generate relapses in any group at effective treatment doses (Supplementary Fig. S5), however, showing a need to interrogate ALK expression in resistant tumors before attempting discontinuous dosing (see Discussion).

Discussion

ALK-kinase inhibition is an important new treatment modality for the subset of NSCLC cases containing ALK rearrangements, but median progression-free survival has ranged from 7 to 10 months during treatment with crizotinib or ceritinib (10, 13, 38). Target-independent resistance is common, as target-dependent mechanisms such second-site kinase-domain mutations are detectable in fewer than half of resistant samples and even then activation of alternate signaling may also be present (14, 18, 19). The small number of ALK⁺ ALCL patients treated to date with ALK TKIs has not permitted determination of typical progression-free survival, and resistant clinical samples are not yet available for assessment (16, 17). In this study, we have attempted to predict resistance pathways using laboratory-based selections, an approach that has identified clinically relevant reasons for targeted drug failure in numerous cancer types (39–42).

Our results suggest a much stronger addiction to ALK signaling in ALCL than observed in NSCLC. Multiple-independent selections performed with both crizotinib and ceritinib resulted in upregulation of *NPM-ALK* to permit survival in the presence of inhibitor, and there was no clear evidence of alternate signaling able to bypass it. Even re-selection of cells already selected for resistance once, but which lost resistance in order to avoid the toxic effects of ALK overdose, again generated ALK upregulation (Supplementary Fig. S4). All resistant lines preserved ALK activation in the presence of inhibitor, though preservation was stronger in some than in others (K299 subclones vs. the others in Fig. 2E), whereas STAT3 activation was strongly preserved in all. It is therefore possible additional mechanisms preserving STAT3 activation arose in some cases, though this was not observed after lines were reselected for ability to grow without inhibitor. Either way, we find the effect of ALK signaling intensity on cell survival exists as an inverted U-shaped curve, which we represent schematically in Fig. 6. *NPM-ALK* overexpression associated with genomic amplification in the case of resistant clones derived from Karpas-299 and without amplification in other clones. The consistent results with Karpas-299 suggest this line might have a subpopulation with *NPM-ALK* amplification at baseline. Such population is then most able to upregulate expression from a tolerable prosurvival baseline to the levels necessary to overcome high concentrations of inhibitor. Even in the resistant *NPM-ALK*-amplified K299-CR1000 clone, however, a subpopulation without the amplification appears to persist, because it reemerges

Amin et al.

**Figure 5.**

ALK resistance dependence *in vivo*. A, mean tumor burden of mice injected with 10^6 K299-CR1000 cells and treated with vehicle or ceritinib ($n = 5$ per group). B, individual tumor burden of tumor-bearing mice following ceritinib discontinuation and subsequent resumption. C-F, viability assays (C), proliferation (D), copy-number (E), and mRNA expression (F) using cells taken from mice 1 and 3 before resumption of ceritinib show the RS phenotype. Cells from mouse 2 were not successfully cultured. Means of technical quadruplicates (C) or independent triplicates (D) or technical triplicates (E and F) \pm SEM.

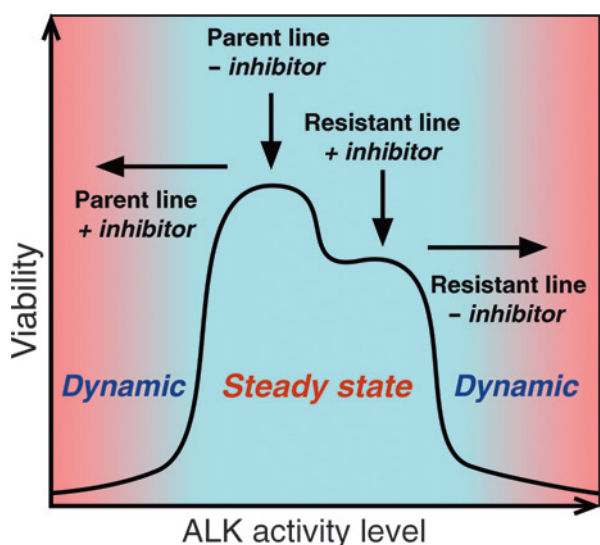


Figure 6.

Schematic of ALK dosage and cell viability. A narrow range of ALK activity promotes cell viability. Addition of TKI to ALK-addicted parent cells or withdrawal of TKI from resistant cells with ALK upregulation drives cells into dynamic states of lost viability, ending in death—but for opposite reasons of ALK signaling dosage.

upon selection for ability to grow again without inhibitor. Another possibility is that the amplification arises extra-chromosomally (e.g., as a double-minute chromosome), which is then lost through chromosomal segregation during selection for growth without inhibitor. Either way, the overexpression without amplification in other resistant clones show additional genetic and/or epigenetic mechanisms can arise to drive overexpression. Gene-expression profiling, unbiased interrogation of signaling through phosphoproteomics, and subsequent functional studies are needed to fully determine these mechanisms and also the mechanisms by which ALK-overdose leads to cell death.

Consistent and reproducible selection for increased NPM-ALK in multiple models of ALK⁺ ALCL we believe may be therapeutically exploitable, with potential application to additional malignancies in which ALK has an established or potential role (4). Therapeutic strategies of inhibitor withdrawal from patients with resistant tumors and up-front schedules of intermittent dosing are approaches carrying far less toxicity and expense than almost any other strategy aimed at overcoming resistance. Our results (Fig. 5) support the former in cases when ALK overexpression is suspected or, preferably, can be specifically detected. Unlike similar results reported recently for BRAF-driven melanoma (43); however, we did not prolong control in the up-front setting with intermittent dosing (Supplementary Fig. S5). These results, however, do not fully interrogate the strategy since no relapses were observed, which is out of line with expected patient experience, especially in those receiving ALK inhibitors as salvage therapy. Major progress toward producing a phenotypically accurate murine model of ALK⁺ ALCL came recently with demonstration that CRISPR/CAS9-mediated chromosomal breaks can generate NPM-ALK in murine fibroblasts (44). The same report showed retroviral introduction of guide strands generating breaks for EML4-ALK into mouse lungs generated a highly accurate model of ALK⁺ NSCLC. Efforts are underway by several groups including ours to apply these techniques in generation of a new model for ALK⁺ ALCL.

Evaluation of up-front intermittent dosing and discontinuous dosing in the setting of acquired resistance when such a system becomes available are justified by our findings. It also will permit studies of the mechanisms of ALK-overdose toxicity and of non-amplification-driven NPM-ALK overexpression in a physiologically accurate immunocompetent model system.

Important questions raised by our data include those of broader applicability. In lung cancer, EML4-ALK copy-number gain and increased expression are reported in association with crizotinib resistance (18, 19). There are recent case reports of ALK⁺ NSCLC patients who became refractory to crizotinib obtaining secondary responses upon re-challenge after a period off the drug (45, 46). Both patients, however, received chemotherapy upon initial crizotinib discontinuation, so we do not know if ALK overdose was present or might have led to spontaneous regressions if they had been observed without therapy. Another case series found continuing crizotinib treatment despite progression led to higher performance status than discontinuation (47), but no study has addressed the question of whether therapy interruption may benefit some patients based on the particular resistance mechanism(s) present in their tumors. In other cancers with known or potential ALK activation, evaluation of ALK inhibition is at early stages with results largely unreported. We encourage careful evaluation for changes in ALK signaling dosage during ALK inhibitor therapy in ongoing and planned trials. Patients who come off therapy and subsequently experience regression should be assessed for the potential role of ALK overdose in these findings.

In sum, ALK activity can exist as a double-edged sword for cancer cells. Those tumors that are most addicted to its activities for continued proliferation correspondingly are most prone to select for higher expression to bypass its inhibition. Interruption of inhibition would then provide a new way of prolonging tumor control as the other edge of the sword comes into play.

Disclosure of Potential Conflicts of Interest

S.D. Puvvada has received speakers bureau honoraria from Seattle Genetics and is a consultant/advisory board member for Pharmacyclics. No potential conflicts of interest were disclosed by the other authors.

Authors' Contributions

Conception and design: A.D. Amin, L. Cuyugan, J.H. Schatz
Development of methodology: A.D. Amin, W.S. Liang, M.J. Groysman, J. Adkins, Y.A. Lussier, J.H. Schatz
Acquisition of data (provided animals, acquired and managed patients, provided facilities, etc.): A.D. Amin, S.S. Rajan, W.S. Liang, P. Pongtornpipat, M.J. Groysman, E.O. Tapia, T.L. Peters, L. Cuyugan, J. Adkins, L.M. Rimsza, J.H. Schatz
Analysis and interpretation of data (e.g., statistical analysis, biostatistics, computational analysis): A.D. Amin, W.S. Liang, M.J. Groysman, Y.A. Lussier, J.H. Schatz
Writing, review, and/or revision of the manuscript: A.D. Amin, M.J. Groysman, L.M. Rimsza, Y.A. Lussier, S.D. Puvvada, J.H. Schatz
Administrative, technical, or material support (i.e., reporting or organizing data, constructing databases): A.D. Amin, P. Pongtornpipat, Y.A. Lussier
Study supervision: A.D. Amin, J.H. Schatz
Other (assistance in obtaining drug): S.D. Puvvada

Acknowledgments

The authors thank Emanuela Colombo (University of Milano, Milan, Italy) for generously sending the pMIG-NPM-ALK plasmid to us. The authors also thank Denise Olivas-Castillo and Shobana Sekar (Translational Genomics Research Institute, Phoenix, AZ) for their technical expertise for the targeted

Amin et al.

selection and sequencing experiments. The authors especially thank Bethany Skovan, Gillian Paine-Murrieta, and Erica Sontz (Experimental Mouse Shared Service, University of Arizona, Tucson, AZ) for their help and support in conducting any *in vivo* studies.

Grant Support

This work was supported by the NIH/NCI (1R01CA190696-01; J.H. Schatz), University of Arizona Bio5 Institute and Cancer Center (J.H. Schatz), the

Lymphoma Research Foundation (J.H. Schatz), and Translational Genomics Research Institute (W.S. Liang, L. Cuyugan, J. Adkins).

The costs of publication of this article were defrayed in part by the payment of page charges. This article must therefore be hereby marked *advertisement* in accordance with 18 U.S.C. Section 1734 solely to indicate this fact.

Received November 24, 2014; revised April 23, 2015; accepted May 1, 2015; published OnlineFirst May 27, 2015.

References

- Iwahara T, Fujimoto J, Wen D, Cupples R, Bucay N, Arakawa T, et al. Molecular characterization of ALK, a receptor tyrosine kinase expressed specifically in the nervous system. *Oncogene* 1997;14:439–49.
- Vernersson E, Khoo NK, Henriksson ML, Roos G, Palmer RH, Hallberg B. Characterization of the expression of the ALK receptor tyrosine kinase in mice. *Gene Expr Patterns* 2006;6:448–61.
- Crockett DK, Lin Z, Elenitoba-Johnson KS, Lim MS. Identification of NPM-ALK interacting proteins by tandem mass spectrometry. *Oncogene* 2004;23:2617–29.
- Hallberg B, Palmer RH. Mechanistic insight into ALK receptor tyrosine kinase in human cancer biology. *Nat Rev Cancer* 2013;13:685–700.
- McDonnell SR, Hwang SR, Rolland D, Murga-Zamalloa C, Basrur V, Conlon KP, et al. Integrated phosphoproteomic and metabolomic profiling reveals NPM-ALK-mediated phosphorylation of PKM2 and metabolic reprogramming in anaplastic large cell lymphoma. *Blood* 2013;122:958–68.
- Pearson JD, Lee JK, Bacani JT, Lai R, Ingham RJ. NPM-ALK: the prototypic member of a family of oncogenic fusion tyrosine kinases. *J Signal Transduct* 2012;2012:123253.
- Morris SW, Kirstein MN, Valentine MB, Dittmer KG, Shapiro DN, Saltman DL, et al. Fusion of a kinase gene, ALK, to a nucleolar protein gene, NPM, in non-Hodgkin's lymphoma. *Science* 1994;263:1281–4.
- Soda M, Choi YL, Enomoto M, Takada S, Yamashita Y, Ishikawa S, et al. Identification of the transforming EML4-ALK fusion gene in non-small-cell lung cancer. *Nature* 2007;448:561–6.
- Rikova K, Guo A, Zeng Q, Possemato A, Yu J, Haack H, et al. Global survey of phosphotyrosine signaling identifies oncogenic kinases in lung cancer. *Cell* 2007;131:1190–203.
- Kwak EL, Bang YJ, Camidge DR, Shaw AT, Solomon B, Maki RG, et al. Anaplastic lymphoma kinase inhibition in non-small-cell lung cancer. *N Engl J Med* 2010;363:1693–703.
- Shaw AT, Kim DW, Nakagawa K, Seto T, Crino L, Ahn MJ, et al. Crizotinib versus chemotherapy in advanced ALK-positive lung cancer. *N Engl J Med* 2013;368:2385–94.
- Solomon BJ, Mok T, Kim DW, Wu YL, Nakagawa K, Mekhail T, et al. First-line crizotinib versus chemotherapy in ALK-positive lung cancer. *N Engl J Med* 2014;371:2167–77.
- Shaw AT, Kim DW, Mehra R, Tan DS, Felip E, Chow LQ, et al. Ceritinib in ALK-rearranged non-small-cell lung cancer. *N Engl J Med* 2014;370:1189–97.
- Peters S, Taron M, Bubendorf L, Blackhall F, Stahel R. Treatment and detection of ALK-rearranged NSCLC. *Lung Cancer* 2013;81:145–54.
- Vose J, Armitage J, Weisenburger D. International peripheral T-cell and natural killer/T-cell lymphoma study: pathology findings and clinical outcomes. *J Clin Oncol* 2008;26:4124–30.
- Mossé YP, Lim MS, Voss SD, Wilner K, Ruffner K, Laliberte J, et al. Safety and activity of crizotinib for paediatric patients with refractory solid tumours or anaplastic large-cell lymphoma: a Children's Oncology Group phase 1 consortium study. *Lancet Oncol* 2013;14:472–80.
- Gambacorti Passerini C, Farina F, Stasia A, Redaelli S, Ceccon M, Mologni L, et al. Crizotinib in advanced, chemoresistant anaplastic lymphoma kinase-positive lymphoma patients. *J Natl Cancer Inst* 2014;106:djt378.
- Katayama R, Shaw AT, Khan TM, Mino-Kenudson M, Solomon BJ, Halmos B, et al. Mechanisms of acquired crizotinib resistance in ALK-rearranged lung cancers. *Sci Transl Med* 2012;4:120ra17.
- Doebbele RC, Pilling AB, Aisner DL, Kutateladze TG, Le AT, Weickhardt AJ, et al. Mechanisms of resistance to crizotinib in patients with ALK gene rearranged non-small cell lung cancer. *Clin Cancer Res* 2012;18:1472–82.
- Liang WS, Aldrich J, Tembe W, Kurdoglu A, Cherni I, Phillips L, et al. Long insert whole genome sequencing for copy number variant and translocation detection. *Nucleic Acids Res* 2014;42:e8.
- Onciu M, Behm FG, Downing JR, Shurtleff SA, Raimondi SC, Ma Z, et al. ALK-positive plasmablastic B-cell lymphoma with expression of the NPM-ALK fusion transcript: report of 2 cases. *Blood* 2003;102:2642–4.
- Li H, Durbin R. Fast and accurate short read alignment with Burrows-Wheeler transform. *Bioinformatics* 2009;25:1754–60.
- Li H, Handsaker B, Wysoker A, Fennell T, Ruan J, Homer N, et al. The Sequence Alignment/Map format and SAMtools. *Bioinformatics* 2009;25:2078–9.
- McKenna A, Hanna M, Banks E, Sivachenko A, Cibulskis K, Kernysky A, et al. The Genome Analysis Toolkit: a MapReduce framework for analyzing next-generation DNA sequencing data. *Genome Res* 2010;20:1297–303.
- Christoforides A, Carpten JD, Weiss GJ, Demeure MJ, VonHoff DD, Craig DW. Identification of somatic mutations in cancer through Bayesian-based analysis of sequenced genome pairs. *BMC Genomics* 2013;14:302.
- Cibulskis K, Lawrence MS, Carter SL, Sivachenko A, Jaffe D, Sougnez C, et al. Sensitive detection of somatic point mutations in impure and heterogeneous cancer samples. *Nat Biotechnol* 2013;31:213–9.
- Saunders CT, Wong WS, Swamy S, Becq J, Murray LJ, Cheetham RK, Strelka: accurate somatic small-variant calling from sequenced tumor-normal sample pairs. *Bioinformatics* 2012;28:1811–7.
- Marsilje TH, Pei W, Chen B, Lu W, Uno T, Jin Y, et al. Synthesis, structure-activity relationships, and *in vivo* efficacy of the novel potent and selective anaplastic lymphoma kinase (ALK) inhibitor 5-chloro-N2-(2-isopropoxy-5-methyl-4-(piperidin-4-yl)phenyl)-N4-(2-(isopropylsulfonyl)phenyl)pyrimidine-2,4-diamine (LDK378) currently in phase 1 and phase 2 clinical trials. *J Med Chem* 2013;56:5675–90.
- Bonvini P, Dalla Rosa H, Vignes N, Rosolen A. Ubiquitination and proteasomal degradation of nucleophosmin-anaplastic lymphoma kinase induced by 17-allylamino-demethoxygeldanamycin: role of the co-chaperone carboxyl heat shock protein 70-interacting protein. *Cancer Res* 2004;64:3256–64.
- Chiarle R, Simmons WJ, Cai H, Dhall G, Zamo A, Raz R, et al. Stat3 is required for ALK-mediated lymphomagenesis and provides a possible therapeutic target. *Nat Med* 2005;11:623–9.
- Piva R, Agnelli L, Pellegrino E, Todoerti K, Grosso V, Tamagno I, et al. Gene expression profiling uncovers molecular classifiers for the recognition of anaplastic large-cell lymphoma within peripheral T-cell neoplasms. *J Clin Oncol* 2010;28:1583–90.
- Mossé YP, Laudenslager M, Longo L, Cole KA, Wood A, Attiyeh EF, et al. Identification of ALK as a major familial neuroblastoma predisposition gene. *Nature* 2008;455:930–5.
- Friboulet L, Li N, Katayama R, Lee CC, Gainor JF, Crystal AS, et al. The ALK inhibitor ceritinib overcomes crizotinib resistance in non-small cell lung cancer. *Cancer Discov* 2014;4:662–73.
- Zhang S, Wang F, Keats J, Zhu X, Ning Y, Wardwell SD, et al. Crizotinib-resistant mutants of EML4-ALK identified through an accelerated mutagenesis screen. *Chem Biol Drug Design* 2011;78:999–1005.
- Zdzalik D, Dymek B, Gryglewicz P, Gunerka P, Bujak A, Lamparska-Przybylska M, et al. Activating mutations in ALK kinase domain confer resistance to structurally unrelated ALK inhibitors in NPM-ALK-positive anaplastic large-cell lymphoma. *J Cancer Res Clin Oncol* 2014;140:589–98.
- Chand D, Yamazaki Y, Ruuth K, Schonherr C, Martinsson T, Kogner P, et al. Cell culture and *Drosophila* model systems define three classes of anaplastic lymphoma kinase mutations in neuroblastoma. *Dis Mod Mech* 2013;6:373–82.

37. Algate PA, Steelman LS, Mayo MW, Miyajima A, McCubrey JA. Regulation of the interleukin-3 (IL-3) receptor by IL-3 in the fetal liver-derived FL5.12 cell line. *Blood* 1994;83:2459–68.
38. Shaw AT, Engelman JA. ALK in lung cancer: past, present, and future. *J Clin Oncol* 2013;31:1105–11.
39. Engelman JA, Zejnullahu K, Mitsudomi T, Song Y, Hyland C, Park JO, et al. MET amplification leads to gefitinib resistance in lung cancer by activating ERBB3 signaling. *Science* 2007;316:1039–43.
40. Corcoran RB, Dias-Santagata D, Bergethon K, Iafrate AJ, Settleman J, Engelman JA. BRAF gene amplification can promote acquired resistance to MEK inhibitors in cancer cells harboring the BRAF V600E mutation. *Sci Signaling* 2010;3:ra84.
41. Poulidakos PI, Persaud Y, Janakiraman M, Kong X, Ng C, Moriceau G, et al. RAF inhibitor resistance is mediated by dimerization of aberrantly spliced BRAF(V600E). *Nature* 2011;480:387–90.
42. Yonesaka K, Zejnullahu K, Okamoto I, Satoh T, Cappuzzo F, Souglakos J, et al. Activation of ERBB2 signaling causes resistance to the EGFR-directed therapeutic antibody cetuximab. *Sci Transl Med* 2011;3:99ra86.
43. Das Thakur M, Salangsang F, Landman AS, Sellers WR, Pryer NK, Levesque MP, et al. Modelling vemurafenib resistance in melanoma reveals a strategy to forestall drug resistance. *Nature* 2013;494:251–5.
44. Maddalo D, Manchado E, Concepcion CP, Bonetti C, Vidigal JA, Han YC, et al. In vivo engineering of oncogenic chromosomal rearrangements with the CRISPR/Cas9 system. *Nature* 2014;516:423–7.
45. Browning ET, Weickhardt AJ, Camidge DR. Response to crizotinib rechallenge after initial progression and intervening chemotherapy in ALK lung cancer. *J Thorac Oncol* 2013;8:e21.
46. Schrödl K, von Schilling C, Tufman A, Huber RM, Gamarra F. Response to chemotherapy, reexposure to crizotinib and treatment with a novel ALK inhibitor in a patient with acquired crizotinib resistance. *Respiration* 2014;88:262–4.
47. Ou SH, Janne PA, Bartlett CH, Tang Y, Kim DW, Otterson GA, et al. Clinical benefit of continuing ALK inhibition with crizotinib beyond initial disease progression in patients with advanced ALK-positive NSCLC. *Ann Oncol* 2014;25:415–22.

Cancer Research

The Journal of Cancer Research (1916–1930) | The American Journal of Cancer (1931–1940)

Evidence Suggesting That Discontinuous Dosing of ALK Kinase Inhibitors May Prolong Control of ALK⁺ Tumors

Amit Dipak Amin, Soumya S. Rajan, Winnie S. Liang, et al.

Cancer Res 2015;75:2916-2927. Published OnlineFirst May 27, 2015.

Updated version Access the most recent version of this article at:
doi:[10.1158/0008-5472.CAN-14-3437](https://doi.org/10.1158/0008-5472.CAN-14-3437)

Supplementary Material Access the most recent supplemental material at:
<http://cancerres.aacrjournals.org/content/suppl/2015/05/28/0008-5472.CAN-14-3437.DC1.html>

Cited articles This article cites 47 articles, 20 of which you can access for free at:
<http://cancerres.aacrjournals.org/content/75/14/2916.full.html#ref-list-1>

E-mail alerts [Sign up to receive free email-alerts](#) related to this article or journal.

Reprints and Subscriptions To order reprints of this article or to subscribe to the journal, contact the AACR Publications Department at pubs@aacr.org.

Permissions To request permission to re-use all or part of this article, contact the AACR Publications Department at permissions@aacr.org.